NAVAL POSTGRADUATE SCHOOL

MONTEREY, CALIFORNIA

THESIS

USE OF CARBON NANO-FIBER FOAMS AS STRAIN GAUGES TO DETECT CRACK PROPAGATION

by

Ervin N. Mercado

June 2015

Thesis Advisor: Claudia C. Luhrs
Co-Advisor: Jonathan Phillips

THIS PAGE INTENTIONALLY LEFT BLANK

REPORT DOCUMENTATION PAGE

Form Approved OMB No. 0704–0188

1. AGENCY USE ONLY *(Leave blank)*	**2. REPORT DATE** June 2015	**3. REPORT TYPE AND DATES COVERED** Master's Thesis

4. TITLE AND SUBTITLE
USE OF CARBON NANO-FIBER FOAMS AS STRAIN GAUGES TO DETECT CRACK PROPAGATION

5. FUNDING NUMBERS

6. AUTHOR(S) Ervin N. Mercado

7. PERFORMING ORGANIZATION NAME(S) AND ADDRESS(ES)
Naval Postgraduate School
Monterey, CA 93943–5000

8. PERFORMING ORGANIZATION REPORT NUMBER

9. SPONSORING /MONITORING AGENCY NAME(S) AND ADDRESS(ES)
N/A

10. SPONSORING/MONITORING AGENCY REPORT NUMBER

11. SUPPLEMENTARY NOTES The views expressed in this thesis are those of the author and do not reflect the official policy or position of the Department of Defense or the U.S. Government. IRB Protocol number ____N/A____.

12a. DISTRIBUTION / AVAILABILITY STATEMENT
Approved for public release; distribution is unlimited

12b. DISTRIBUTION CODE

13. ABSTRACT (maximum 200 words)

This thesis focuses on testing the feasibility of using carbon nanofiber foams as strain gauge material to detect crack propagation in aluminum structures. We produced the tridimensional carbon nanofiber foams using a process that exposed palladium catalyst particles to a fuel rich oxygen/ethylene mixture at moderate temperatures in a tubular furnace. The microstructure of the foam generated was characterized using a scanning electron microscope to determine diameter and distribution of the fibers within the foam. Sections of the foam, electrically isolated, were attached to aluminum tensile specimens. Simultaneous mechanical and electrical measurements were conducted on the aluminum-foam fixtures. The mechanism responsible for the conductivity values seems to be related to the number of contacts established between all fibers as the foam was compressed or stretched during tensile tests, as opposed to the electrical properties of the individual fibers. The design of the foam sensor and the way it is attached to the aluminum plates presented challenges that will need to be further addressed. The data showed a correlation between strain levels in the aluminum probes and the resistivity detected in the foam, confirming that the later can be employed as a sensor to monitor the structural integrity of the former.

14. SUBJECT TERMS carbon nano-fiber foam, crack propagation, strain gauges	**15. NUMBER OF PAGES** 71
	16. PRICE CODE

17. SECURITY CLASSIFICATION OF REPORT	**18. SECURITY CLASSIFICATION OF THIS PAGE**	**19. SECURITY CLASSIFICATION OF ABSTRACT**	**20. LIMITATION OF ABSTRACT**
Unclassified	Unclassified	Unclassified	UU

NSN 7540–01–280–5500

Standard Form 298 (Rev. 2–89)
Prescribed by ANSI Std. 239–18

THIS PAGE INTENTIONALLY LEFT BLANK

Approved for public release; distribution is unlimited

USE OF CARBON NANO-FIBER FOAMS AS STRAIN GAUGES TO DETECT CRACK PROPAGATION

Ervin N. Mercado
Lieutenant, United States Navy
B.S., United States Naval Academy, 2008

Submitted in partial fulfillment of the
requirements for the degree of

MASTER OF SCIENCE IN MECHANICAL ENGINEERING

from the

NAVAL POSTGRADUATE SCHOOL
June 2015

Author: Ervin N. Mercado

Approved by: Claudia C. Luhrs
Thesis Advisor

Jonathan Phillips
Co-Advisor

Garth V. Hobson
Chair, Department of Mechanical and Aerospace Engineering

THIS PAGE INTENTIONALLY LEFT BLANK

ABSTRACT

This thesis focuses on testing the feasibility of using carbon nanofiber foams as strain gauge material to detect crack propagation in aluminum structures. We produced the tridimensional carbon nanofiber foams using a process that exposed palladium catalyst particles to a fuel rich oxygen/ethylene mixture at moderate temperatures in a tubular furnace. The microstructure of the foam generated was characterized using a scanning electron microscope to determine diameter and distribution of the fibers within the foam. Sections of the foam, electrically isolated, were attached to aluminum tensile specimens. Simultaneous mechanical and electrical measurements were conducted on the aluminum-foam fixtures. The mechanism responsible for the conductivity values seems to be related to the number of contacts established between all fibers as the foam was compressed or stretched during tensile tests, as opposed to the electrical properties of the individual fibers. The design of the foam sensor and the way it is attached to the aluminum plates presented challenges that will need to be further addressed. The data showed a correlation between strain levels in the aluminum probes and the resistivity detected in the foam, confirming that the later can be employed as a sensor to monitor the structural integrity of the former.

THIS PAGE INTENTIONALLY LEFT BLANK

TABLE OF CONTENTS

THIS PAGE INTENTIONALLY LEFT BLANK

LIST OF FIGURES

LIST OF TABLES

THIS PAGE INTENTIONALLY LEFT BLANK

LIST OF ACRONYMS AND ABBREVIATIONS

Al	Aluminum
CFF	Carbon Nano-Fiber Foam
CNT	Carbon Nano-Tube
Cu	Copper
GF	Gauge Factor
GSD	Graphitic Structures by Design
IGSCC	Intergranular Stress Corrosion Cracking
MPa	Mega Pascals
Mg	Magnesium
nm	Nanometer
N	Newton
Pd	Palladium
PDMS	Polydimethylsiloxane
SCC	Stress Corrosion Cracking
SCCM	Standard Cubic Centimeter per minute
SEM	Scanning Electron Microscope
SHM	Structural Health Monitoring
SWCNT	Single Wall Carbon Nano-tube
UHP	Ultra High Purity
μm	Micrometer
%wt	Weight Percent

THIS PAGE INTENTIONALLY LEFT BLANK

ACKNOWLEDGMENTS

In the development of this thesis, the direction and guidance was provided by Dr. Claudia Luhrs and Dr. Jonathan Phillips. Without their help and instruction through the entire process, I would not have been able to complete the amount of work that I had set out to accomplish. They both have played an integral part in furthering my professional and graduate development throughout my time at NPS.

Learning how to use SEM and achieve images played an important part of my thesis. I would like to thank Dr. Sarath Menon for his professional research expertise and guidance.

Learning how to use the INSTRON Tensile machine and executing the experiments successfully was a huge undertaking, and would not have been possible without the assistance and guidance of Dr. Chanman Park.

Thanks to all my fellow ME cohort (Doug Miller, Karima Greenaway, Will Curtin, Corey Wagner, Thomas Samaras, Jose Alberti, Ben Carroll, Christopher Deigel, and Bob Riley) who have helped me survive this challenging and rewarding graduate endeavor. I would not have gone this far without your talents and your willingness to help a fellow shipmate/classmate.

Finally, my thanks to my family and closest friends who have supported me through the entire process. Without them, I would not have the motivation and determination to grind through and overcome this beautiful struggle.

THIS PAGE INTENTIONALLY LEFT BLANK

I. INTRODUCTION

A. MOTIVATION

The U.S. Navy's use of aluminum for vessel structures has grown in recent years, with several classes of ships using aluminum as a structural material for their hulls, deckhouses, and superstructures, (Figure 1). Aluminum is approximately one third the density of steel with comparable strength and weldability, making it a viable material choice. Specifically, the 5000 series aluminum alloys have been considered a good choice for marine applications due to their high general corrosion resistance compared to other aluminum alloys [1]. Primarily, Al5083 and Al5456 are used in ship construction because of their many desirable attributes, including high strength-to-weight ratios, excellent corrosion-resistance and excellent as-welded strength [2–4]. Aluminum alloys have several limitations not found in steels that must be addressed and mitigated to prolong a ship's operational service life. Some of the failure modes encountered in aluminum structures are related to sensitization, stress corrosion cracking (SCC), fatigue and re-cracking of repaired sections due to residual stress in the welds, among others [2]. These failure mechanisms affect naval combatants ability to remain a strategic national defense asset by threatening its combat requirement to meet high, operational demands and survivability.

Figure 1. Examples of U.S. naval vessels built using marine-grade aluminum in their superstructures and/or hulls. (Left) guided-missile cruiser (CG 52), from [5]. (Right) littoral combat ship (LCS 1), from [6].

1. Aluminum Sensitization

Sensitization occurs as function of both the material's magnesium (Mg) content and the amount of time it remains in a heated environment. When an aluminum alloy contains more than 3 wt% Mg, as is the case of Al5083 (4.5wt%) and AL5456 (5.1wt%), and is exposed to temperatures above 70°C over the course of many years, the aluminum alloy will become sensitized [7–9]. Such behavior can be better understood by analyzing the Al-Mg phase diagram (Figure 2), where the different phases, depending on composition and temperature, are presented. The sensitization of the material occurs as Mg migrates out of the solid solution and forms beta phase (Mg_2Al_3) at the grain boundaries (Figure 3). The beta phase precipitation at the grain boundaries acts as an anodic area to the Mg-depleted interior of the grain, causing a corrosive chemical reaction at the grain boundaries [3] ,[7]. This causes the Al-Mg alloy's grain boundaries to be susceptible to corrosion, thus meeting one of the three criterions for SCC as shown in Figure 4.

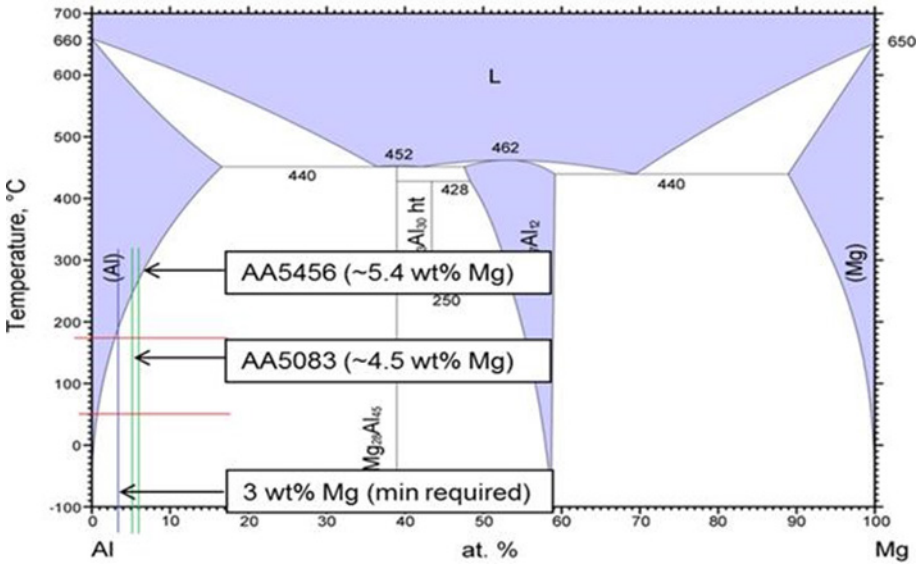

Figure 2. Aluminum-magnesium phase diagram with 3 wt% Mg, Al5083, and Al5456 highlighted, after [4], [10].

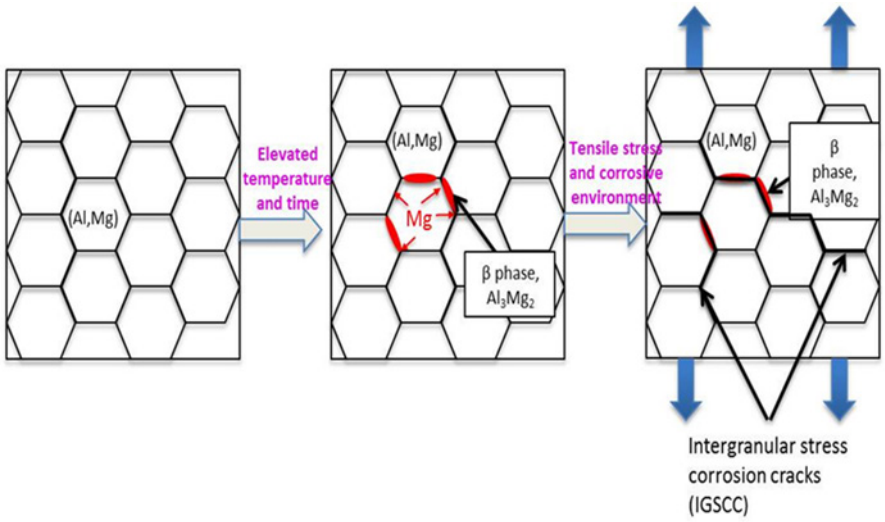

Figure 3. Schematic illustrating sensitization outcome on a 5000 series aluminum-alloy, from [11].

2. Stress Corrosion Cracking

In order for SCC to occur in aluminum alloy, the following three conditions must be met: a susceptible material, exposure to a corrosive environment, and the presence of a tensile stress; this relationship is delineated in the Venn diagram in Figure 4. In the case of Al5083 and Al5456, when they become sensitized, they are considered susceptible to SCC. This mode of material failure has created a series of costly repair problems in the U.S. Navy. The Ticonderoga class guided missile cruiser superstructure, for example, has been plagued by SCC. Early in their life cycle, all of these ships experienced topside fatigue cracking amidships (see Figure 5), due to high localized stresses as well as cyclic loading leading to fatigue [1], [11]. Maintaining this class of ship has become a primary concern for the Navy in more recent years due to new budgetary restrictions and the additional cost in developing a replacement to this aging class of ship, which is quickly approaching its service life of 36 years [1], [3]. In recent years, Congress and Pentagon officials are working to determine how a maintenance program can extend their originally designed service life. Developing a comprehensive maintenance plan for the Ticonderoga class repairs will also benefit other ship classes being built with similar aluminum alloys to include the U.S. Navy's littoral combat ship [3].

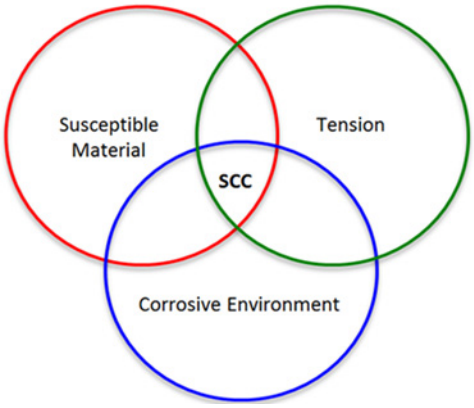

Figure 4. Venn diagram displaying the three factors required for stress corrosion cracking (SCC), from [3].

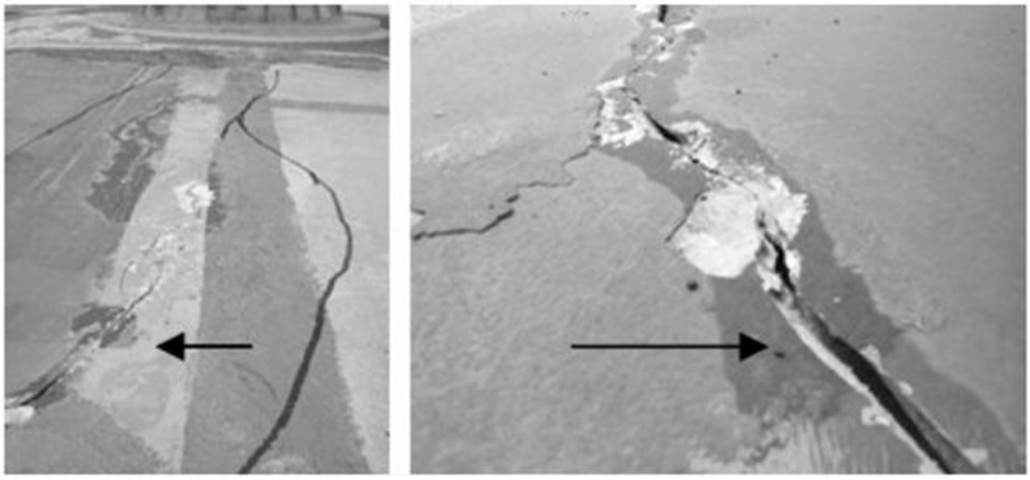

Figure 5. Stress corrosion cracking in Al5456, from [1].

3. Corrosion and Structural Fatigue

Since naval vessels are exposed to corrosive seawater conditions on a daily basis, corrosion fatigue is prone to occur. Corrosion fatigue is the acceleration of the fatigue failure of materials by exposure to a reactive environment. As a failure mode, fatigue crack propagation is the predominant mode of failure in metals and accounts for 90% of failures in all material types [12]. The driving force for most crack propagation on naval vessels is fatigue loading which occurs cyclically as the ship passes over a wave crest.

Ship structural fatigue resulting from cyclic loading, mostly occurs at welds. When a repeated load is heavy enough or applied ample times to cause a fatigue crack,

the crack will start at the point of maximum stress [13]. After a fatigue crack is initiated at a certain level of stress concentration, the crack will act as an additional stress raiser causing crack propagation [13]. The crack propagates with each repetition of the load until the effective cross section is reduced to a point that the remaining portion will fail with the next load cycle.

Overall, corrosion and fatigue cracking are the most prevalent types of structural problems experienced by Navy ships. Each of the damage modes, if not properly monitored and repaired, can potentially lead to disastrous failure or unexpected out-of-service time.

To limit crack propagation in Al structures due to the failure mechanisms mentioned above, sometimes temporary fixes are employed, such as covering of the affected areas with glass reinforced plastics. Such overlays offer sufficient strength for structures to continue being used while providing a water resistance surface [2]. With such repairs in place, however, monitoring further cracks growth is difficult.

4. Structural Health Monitoring

Structural health monitoring (SHM) systems have been proposed as an attempt to identify and model the integrity of the structures over time [2]. This monitoring tool can enhance safety and reduce entire ownership costs of all ships, particularly fast-moving aluminum vessels [14]. These vessels are prone to damage from recurrent and severe wave impact, which have resulted in frequent repairs to local structure due to dishing, buckling, and cracking. A reliable structural health monitoring system can help monitor operational loads, detect performance degradation and structural damage in the earliest stage, diagnostically predict time of potentially structural failure and help enforce corrective actions to secure structural integrity of the ship [14].

Structural health monitoring techniques use sensors to detect small variations in signals such as strain or vibration as a result of damage initiation or crack propagation [15]. The variation in strain distributions often depend on the extent of damage and is often highly localized to damage regions. A strain-based approach can thus be employed

to assess damage by monitoring such localized strain variations on common aluminum structures used in naval vessels [16].

Stress corrosion cracking and fatigue cracking remains the extreme maintenance issue in today's naval ships. SCC and fatigue cracks are often difficult to detect, and may possibly grow to dangerous lengths before they are detected. One possible solution to address this issue is to utilize a strain gauge to monitor for any signs of cracking within the structure. Some of the common SHM that are being used are ultrasonic wave propagation technique, acoustic emission, magnetic field analysis, electrical methods, dye penetrate testing, impact echo testing and X-ray radiography [17]. However, each of these SHM have certain limitations. Most of them are highly susceptible to ambient noise frequency, inaccessible to remote areas, fragile in nature or simple become inadequate once that the structures have been repaired. Today's conventional strain gauge are limited by the durability and sensitivity as a SHM tool to continuously monitor and assess the status of the integrity of a structure with a high level of confidence and reliability.

The contribution of this thesis is to propose a strain-based structural health monitoring system that can help detect and monitor crack growth, in structures that have repaired with polymeric or composite patches. This concept can be easily extended to different sizes of structures at low cost. With an improved strain-based SHM, can help reduce maintenance and inspection cost of structures in today's naval vessels.

B. USE OF CARBON-NANO FIBER STRUCTURES AS STRAIN/PRESSURE SENSORS

Novel materials often lead to novel technologies. This is certainly true of novel forms of carbon, for example, the uniquely high surface area of graphene is being employed to create a new, more energy dense, generation of capacitors [18]. Another example are recent attempts to use carbon fibers and carbon nanotubes to develop sensor devices. Sida Luo created aligned array of SWCNT using several stages of spray coating and sonication techniques, finding that with a large range of tensile strain (20–30%) the CNT's film thickness and microstructure had a compounding effect on the sensor piezoresistive behavior [19]. Su et al. generated carbon microcoils (CMCs) using

chemical vapor disposition process and placed between layers of polydimethylsiloxane (PDMS) with the goal of creating a sensing element, proving that resistance increased with increasing applied pressure between 0–14 kPa [20]. Furthermore, according to Karimov et al. the electromechnical properties of carbon nanotubes could lead to their use of piezoresistors in mechanical sensors such as strain gauges, pressures sensors and accelerometer [16]. They demonstrated this by fabricating a CNT-based pressure sensor and encapsulated in a plastic casing, showing that the resistance of the sensors decreased with increasing pressure.

Another new form of carbon that was developed at NPS are carbon nano-fiber foams. These foams are grown employing the Graphitic Structures by Design (GSD) technique. Another new form of carbon, one partially developed at NPS, are carbon nano-fiber foams. These foams are grown employing the Graphitic Structures by Design (GSD) technique [21]. The method is based on the finding that in fuel rich mixtures of ethylene and oxygen, at moderate temperatures (ca. between 500 and 700°C), graphite structure will form on certain metal catalysts, particularly Pt, Pd, Ni, and Co-Pd mixtures. Of special significance to the present work is the finding that on small metal catalyst particles carbon fibers will rapidly grow. Work at NPS and elsewhere shows many of the features of the fibers, for example the diameter, can be controlled through selection of operating conditions such as temperature and gas flow rate. Moreover, it has been demonstrated, that given adequate time the fibers will “intertwine,” growing together to create a dense mat or “foam” of fibers, known as carbon fiber foams (CFF) [22]. In fact the ultimate dimension of the foam is that of the cavity/mold in which the catalyst particles are placed, process known as Constrained Formation of Fibrous Nanofibers (CoFFiN). Daskam conducted transient and dynamic tests at NPS that proved that CFF material is viscoelastic [23]. Integrated mechanical and electrical testing of samples showed the material to have unique electrical properties appropriate for application as a sensing element of a strain gauge [23].

C. THESIS OBJECTIVES

The following objectives were established for research in this thesis:

1. Determine if carbon-nano fibers foams, based on their electrical response to diverse levels of strain, can be used as gauge sensors to detect crack propagation in aluminum structures.

2. Determine the effective ways of integrating carbon nano-fiber foam, aluminum plate, and adhesive to be used as a strain gauge.

3. Determine which set-up could be best used to perform electrical-mechanical tests.

4. Assess the foam's sensitivity (strain gauge factor) to micro crack propagation.

5. Evaluate the performance of the carbon fiber foam as a sensor and present any advantages over the commercially available sensors.

II. EXPERIMENTAL METHODS

To achieve the objectives stated in the previous chapter, this chapter proceeds in the next order: A) the process of creating the carbon nano-fiber foam (CFF) that will act as the detecting element in a strain gauge, and its microstructural characterization, B) construction of the stain gauge sensors (micro and macro) using the foam, C) continue with machining the specimens of Al5083 to which the foam will be attached, D) describe how the electrical properties of sensors were recorded, E) specify how mechanical tests were conducted. For step C), several variations of CFF strain gauge designs were implemented and are attached to the Al5083 structure, and for F) two types of tensile tests, INSTRON and Micro tensile tester were used to measure the effectiveness of the CFF to detect crack propagation on Al5083 metal structures.

A. FIBER FOAM GENERATION

Samples of CFF were grown using a Constrained Formation of Fibrous Nanostructures (CoFFiN) process, which creates a solid mat of carbon fibers that are intertwined at the nanoscale. The CoFFiN process was developed as a variation of the graphitic structures by design technology as mentioned in the introductory chapter. This novel technique for growing CFF entails partially combust hydrocarbons (ethylene) in the presence of catalyst (e.g., palladium), which allows the CFF to grow until it fills the available space. Thus, growth in a mold can be employed to create any shape of CFF. Under the right conditions of feed composition and temperature (550°C), CFF grows rapidly and follows the form of the mold. The successful generation of CFF is vital to producing the sensing element required to be used in a strain gauge.

1. Precursors and System Setup

The key for the foam generation process is the catalyzed growth of solid carbon structures from radical species formed homogeneously during a fuel rich combustion process. The following growth conditions were implemented: a fuel rich mixture of ethylene and oxygen was flowed over metal particles, spread at the bottom of a steel mold. The mold was placed near the center of 457.2 mm long tube furnace that was held

at 550°C. The use of palladium (Aldrich submicron >99.9) as the CoFFiN catalyst, and the furnace temperature, were selected on the basis of an earlier growth study [23]. That study clearly showed that the Pd based catalysts used at 550°C to grow the CFF produced a 3D object with the mechanical robustness needed in a strain gauge, while Ni particles used in a similar conditions did not [23].

2. Growth Step

For the growth of the carbon nanofiber foam a Pd catalyst was placed into a mold, made of 304 stainless steel, which constrained the volume for the fibers to grow, and promoted their interweaving, as shown in Figure 6. Twenty mg of palladium particles were spread evenly in three equally spaced rows as shown in Figure 7.

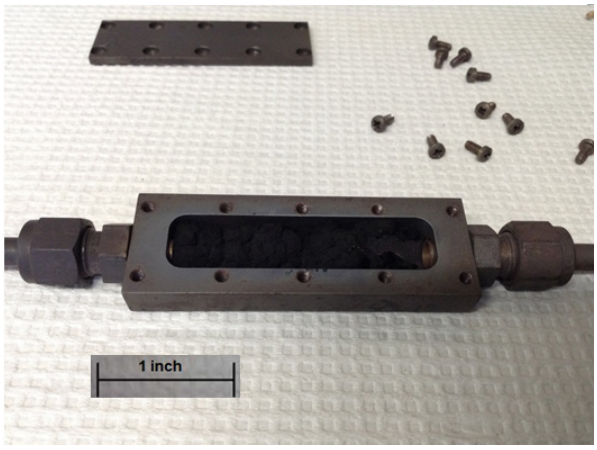

Figure 6. Mold for CFF Growth. The cavity (8.89 mm x 25.4 mm x 57.15 mm) in the stainless steel mold was filled with catalyst, the top fastened, and placed at center of an 457.2 mm long tube furnace.

Figure 7. Catalyst Geometry. Arranging Pd particles in the mold is required to produce homogenous CFF.

This mold chamber was connected to gas flow controller in order to precisely regulate the amount of each gas being passed through the mold and across the catalyst. The gas flow controller can be seen in Figure 8. The mold was then placed into a quartz tube in order to prevent the mold from touching the thermocouple or heating elements inside the furnace. The mold itself was positioned at the center of the tube furnace shown in Figure 9.

The mold/catalyst was thoroughly flushed with UHP Nitrogen at 100 SCCM for 15 minutes to prevent exposure to atmospheric air. The temperature was raised (25 °C/min) to 550°C. At that time the initial reactive gas mixture, composed of ethylene at 15 SCCM and oxygen at 10 SCCM was introduced for 5 minutes. Earlier work shows the initial growth pattern is sustained. Thus, the small diameter fibers generated by the initial gas composition determine the final fiber generation. In order to increase the growth rate, however, the oxygen flow was increased to 15 SCCM after 5 minutes. Finally, after three hours ethylene, oxygen and the furnace were turned off, and the system was allowed to cool. Small fans were used at the ends of the tube to help expedite the cooling process. While cooling the nitrogen gas was maintained at 30 SCCM. Nitrogen was then turned off when the sample has reached room temperature.

Once the single block of CFF was grown it is then removed from the mold and it was attached to Al specimens of two different dimensions to be tested in two different tensile instruments.

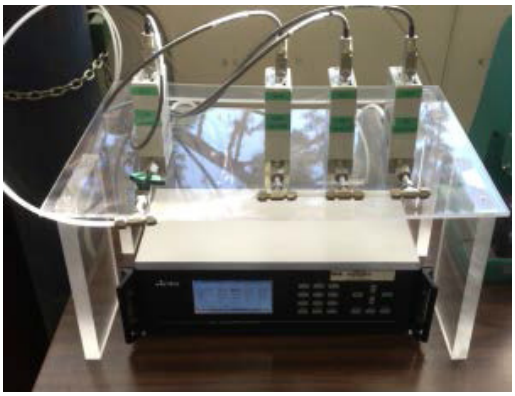

Figure 8. Gas Flow Control. An MKS mass flow controller model MKS 647a (shown), used to control the flow of gasses into the tubular furnace.

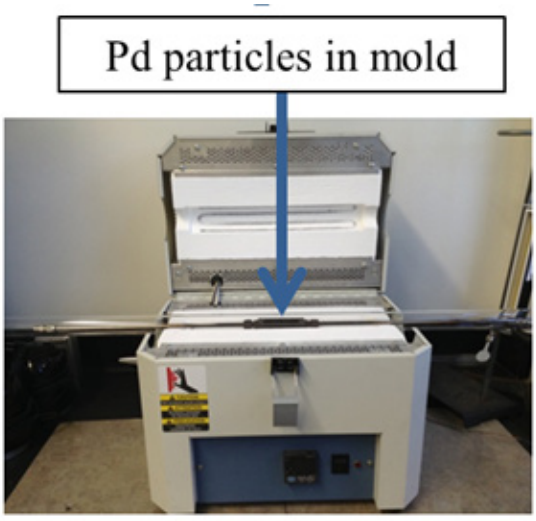

Figure 9. Furnace and mold set-up. For all CFF growth, the mold was filled with catalyst then horizontally in an 457.2 mm x 50.8 mm diameter Lindberg/Blue Mini-Mite Furnace (shown).

3. SEM Microstructural Characterization

In order to characterize the microstructures of the samples a Zeiss Neon 40 High Resolution Scanning electron microscope (SEM) was used. Images of the samples were taken at diverse magnifications and are discussed in the Results chapter. The 30 μm aperture was used with a working distance of five mm. Electron beam currents ranged from 2–20 kV. The images were examined for fiber size and density of fibers within the foam.

B. STRAIN GAUGE SENSOR CONSTRUCTION

Each type of tensile specimen used required a different strain gauge assembly. A certain amount of precision was needed to construct the strain gauge to properly fit within the tensile specimen. The strain gauge assembly for the specimen used on the Microtester contained more miniature size components and takes more time to completely construct (one hour) than the CFF strain gauge assembly (30 minutes) for the INSTRON tensile tests.

1. Micro-sensor Construction

The following components were needed to construct one strain gauge assembly for the Microtester specimen (see Figure 10). Eight of these sensors were successfully constructed for this research.

- CFF
- (3) Polypropylene enclosures (see dimensions in Figure 10)
- Two insulated copper wires
- O-ring caps made out of Ethlyene-Propylene
- Super Glue (Cyanoacrylate, $C_5H_5NO_2$)
- One sheet of aluminum foil
- AL5083 specimen (27.94 mm Length, 2.54 mm width, 10.16 inch thick)

2. Macro-sensor Fabrication

The following components are needed to construct one strain gauge assembly for the INSTRON tensile test specimen (see Figure 11). Six of these sensors were successfully created for this experiment.

- CFF (13.02 mm length x 7 mm width x 2.68 mm thickness)
- Two insulated Al wires
- Nitrocellulose (polymer adhesive)
- AL5083 specimen (220.98 mm length, 7.62 mm width, 6.1468 mm thick)

Figures 12 and 13 illustrate the final design of the two main types of CFF strain gauge assembly used on Microtester and INSTRON tensile test, respectively.

The macro-sensor was constructed to provide a proof of concept using Al specimens of similar thickness than the ones encountered in some applications (0.24 inch). This sensor was not encased in polypropylene, but just electronically isolated from the metal bar using a polymer adhesive. In contrast, the micro-sensor constitutes a prototype of what a sensor device could look like if they were to be produced in large quantities. Moreover, the dimensions of the Aluminum structure, to which it is attached are much smaller, and were meant to determine how sensitive the probe was to micro-cracks. The thickness of the Al in this case was 1.016 mm.

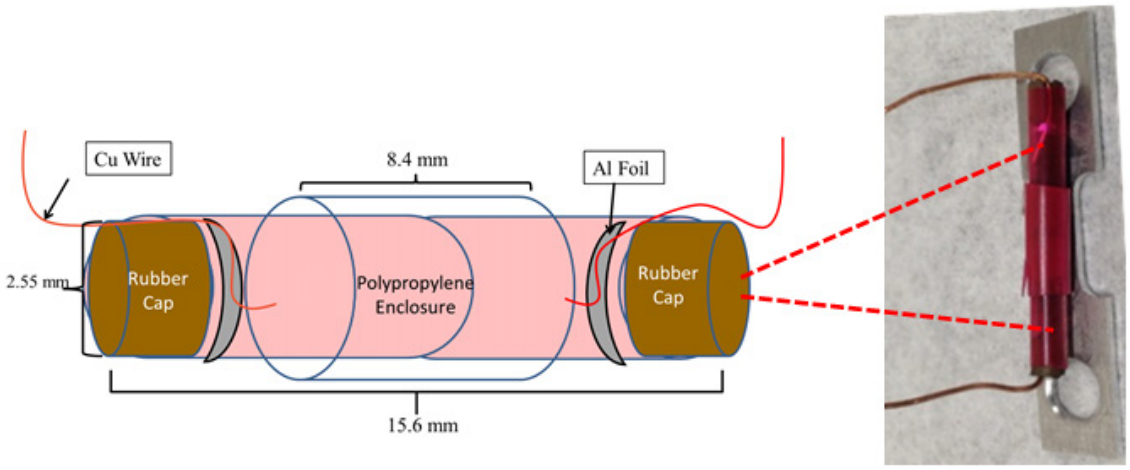

Figure 10. Schematic diagram of CFF strain gauge attached on actual Al5083 Microtester tensile specimen.

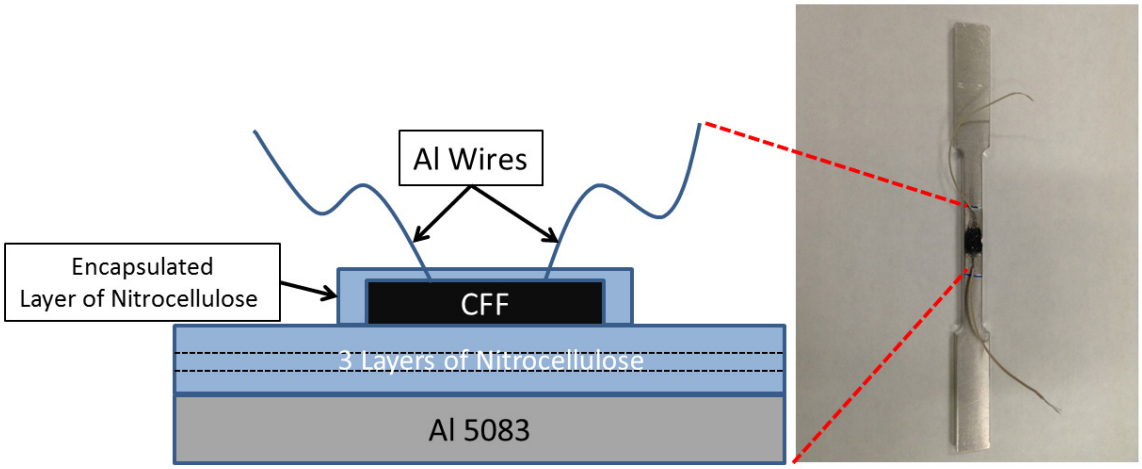

Figure 11. Schematic illustration of CFF strain gauge design attached on Al5083 INSTRON tensile test specimen diagram.

C. SPECIMENS OF AL5083 FOR TENSILE TESTS

Al5083 specimens of two different dimensions were used to measure the effectiveness of the CFF sensing element. The two sizes also reflected the requirements for the Microtester and INSTRON tensile machine. A SERVO CNC 2000 machine mill was used to precisely cut out sheet of Al5083 to fabricate these tensile specimens. The first type is a small specimen used in the Microtester with the following dimensions: 35.56 mm length x 7.62 mm width, (Figure 13).The size restrictions were also imposed

by the available space for the test in the Microtester. The gauge length was 10.06 mm and gauge width was 2.67 mm. The thickness of the specimen was 1.016 mm.

Figure 12. SERVO CNC 2000 Machine Mill used to fabricate the required Al5083 tensile specimens.

The second type is a larger Al5083 specimen with the following dimensions 220.98 mm length, 17.58 mm width, and thickness of 6.15 mm. The gauge length was 88.75 mm and the gauge width was 9.70 mm. This specimen was clamped to conduct a tensile testing utilizing an INSTRON 4507 tensile test machine.

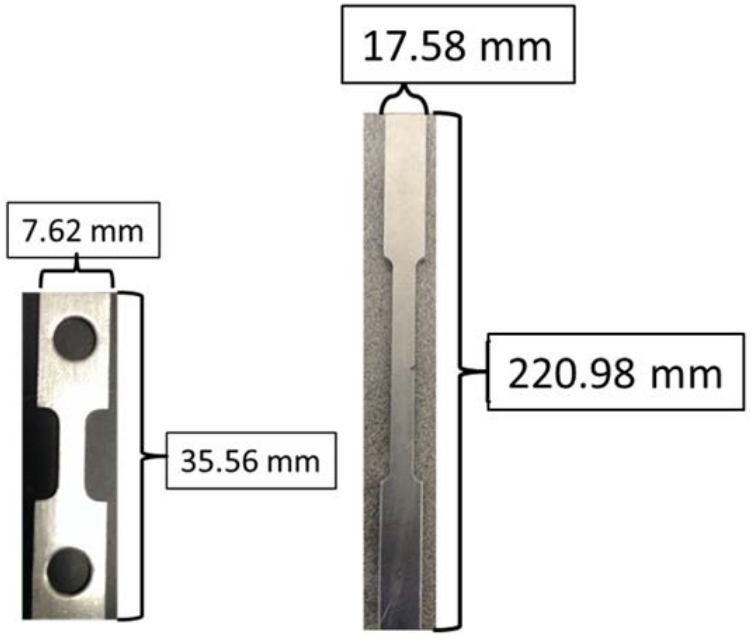

Figure 13. Final product after being machined. (Left) Al5083 Microtester Specimen, 1.02 mm thick. (Right) INSTRON tensile specimen, 6.15 mm thick.

For each type of AL5083 specimen, a unique CFF strain gauge design was attached on the center and near the notch of the tensile specimen. The purpose for this notch is to easily initiate crack propagation on each tensile test run.

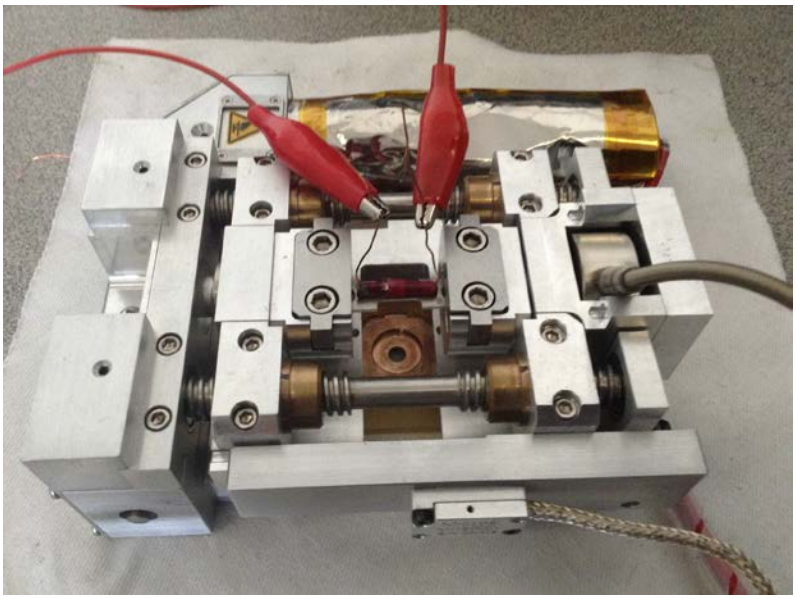

Figure 14. Microtester (compression/tension testers), enables SEM images to be attained of CFF samples under certain levels of stress.

1. Microtester Setup and Procedures

The set-up consisted of Microtester, Agilent 34410A 6 ½ Digit Multi-meter, two copper wires, a computer, Al5083 specimen, timer, and CFF. A unique CFF strain gauge design was specifically fabricated to fit onto the small necking of the AL5083 Microtester specimen as seen in Figure 15.

The Microtester was connected to an MTI data acquisition system, which is connected to a computer running MTEST Quattro program. MTESTQuattro is a computer program which collects, controls, compiles, and stores the data for the Microtester. A digital multi-meter was used to detect the resistance of the CFF strain gauge throughout the duration of the tensile test and was linked to the computer. The resistance was recoded using the Agilent Benchvue software program. A tensile test procedure was created MTESTQuattro program, as followed in Appendix A. The procedure is a programmable set of instructions which tells the Microtester how to perform and record the tensile test. The information consisted of the specimen shape and dimensions, a pre-load of 2.22 N, a pre-load rate of 0.254 mm/min, and a jog rate of 0.0254 mm/min and an overload range of 4,448.22 N.

Prior to running the tensile test procedure, small drops of cyanoacrylate were placed on the top and bottom of strain gauge in order to secure it on the aluminum tensile specimen. Once the strain gauge was affixed, the cyanoacrylate was allowed to dry for 15 minutes. Upon completion, the tensile specimen was placed in the Microtester and the clamps were tightened, Figure 14. Once the specimen was secured, then the Microtester program procedure was initiated. The user recorded the start of tensile test with a timer. Upon fractured of specimen, the test procedure automatically stops. Time of fracture was recorded and the electrical and mechanical data was exported to Microsoft excel program for further analysis.

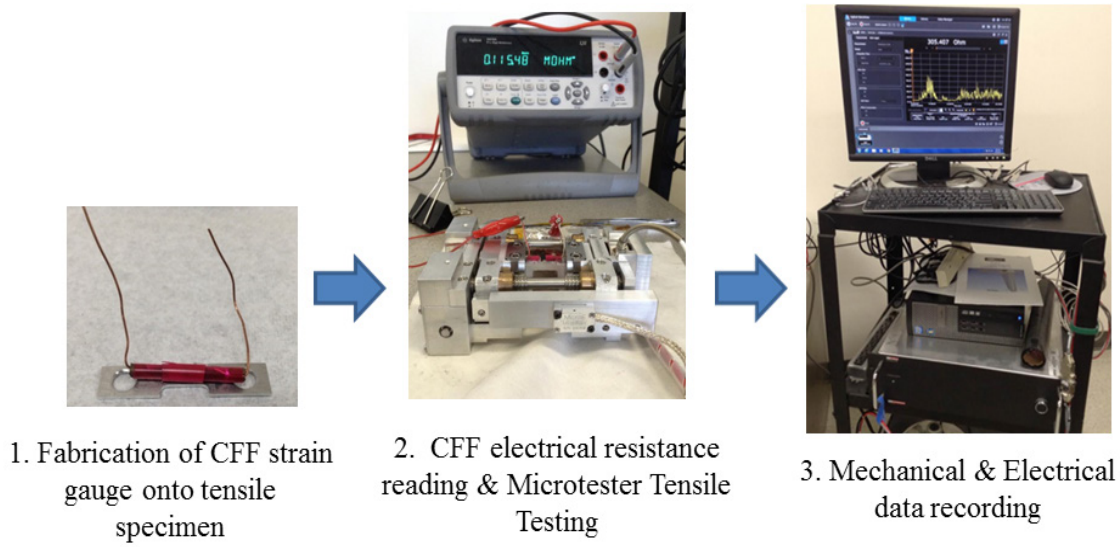

Figure 15. Schematic of experimental method of CFF strain gauge conducted on the Microtester device.

2. INSTRON Tensile Test Setup and Procedures

To determine tensile strength of the larger Al5083 specimen, the INSTRON 4507 tensile tester was used. It has a maximum load of 200 kN (44000 lbs). The INSTRON tester is connected to a computer that contains the INSTRON Blue Hill program, which collects, controls, compiles and stores the data for the tester. The procedures for using the INSTRON Blue Hill program is shown in Appendix B.

The set-up consisted of INSTRON 4507 tensile tester, Agilent 34410A 6½ Digital Multimeter, two aluminum wires, a computer with the installed BLUE HILL program, Al5083 specimen, polymer adhesive, a timer and CFF. A CFF strain gauge design was specifically created to fit onto the middle of the gauge length and near the notch of Al5083 specimen, Figure 16.

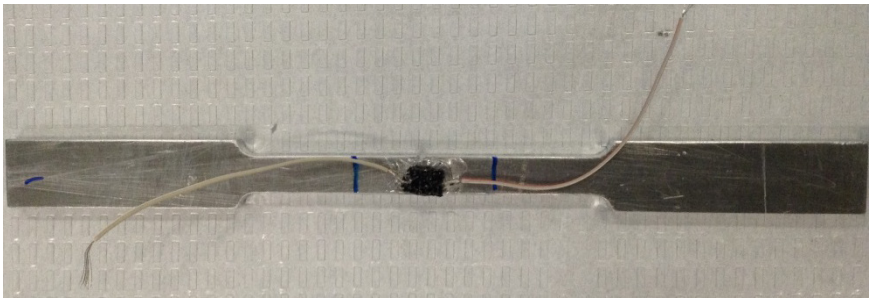

Figure 16. CFF Strain gauge assembly located at the center and near the notch of the tensile specimen.

Once the INSTRON tensile tester machine is activated, a tensile test procedure was created in INSTRON Blue Hill program. The procedure is a programmable set of instructions which tells the INSTRON tester how to perform and record the tensile test. The information consisted of inputting specimen dimensions in terms of its width, thickness, and gauge length. For each run, the following tensile rates were implemented in the INSTRON Blue Hill program: 1 mm/min and 0.7 mm/min.

For each tensile specimen, a square piece of CFF (13.02 mm length x 7 mm width x 2.68 mm thickness) was placed near the notch of the specimen. Prior to placing the CFF onto the specimen, three layers of polymer adhesive coating were applied on center of the gauge length of the specimen. The layers of polymer adhesive were placed on the specimen based on the blue marker position (Figure 16) and 15 minutes was allotted for the adhesive to dry. After three coatings were successfully applied on the specimen, the CFF was placed onto the top of the coating and one layer of polymer adhesion is encapsulated onto the CFF (Figure 16).

The specimen was securely placed within the top and bottom grips of the INSTRON tensile tester. The two wire ends were then connected to the digital multimeter

linked to the Agilent computer program which recorded the resistance of the specimen throughout the tensile test runs as shown in Figure 17.

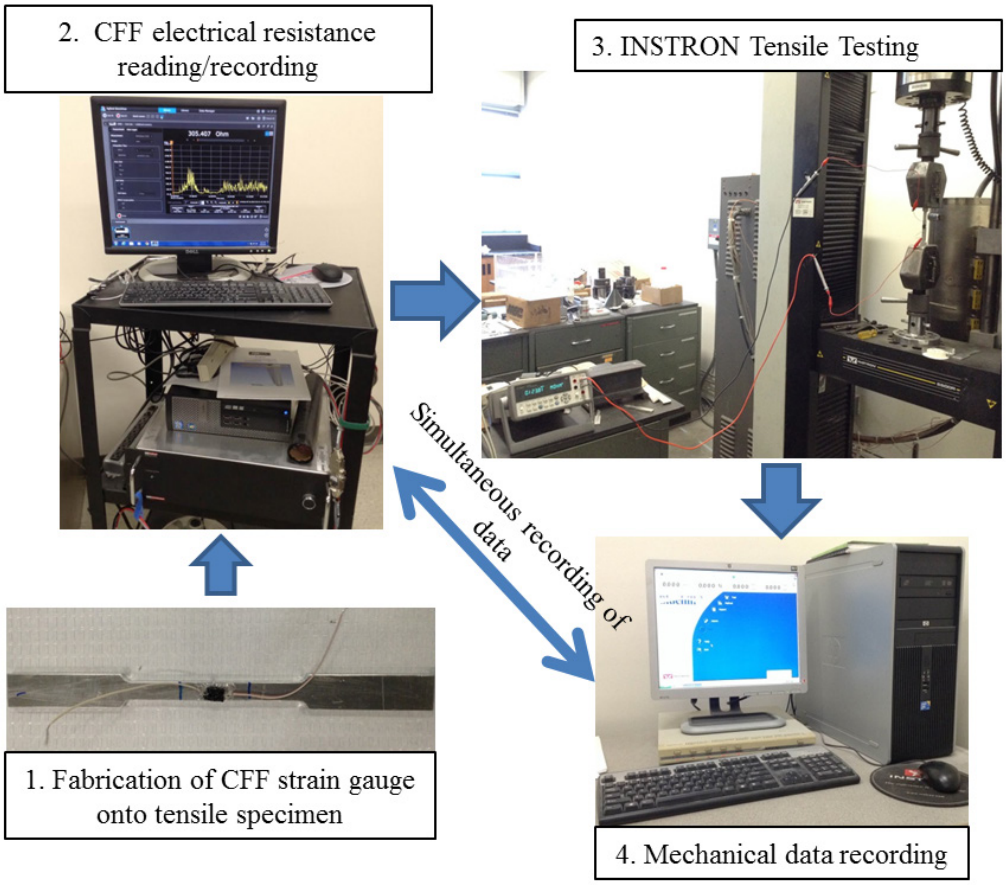

Figure 17. Schematic of experimental method for CFF strain gauge conducted on the INSTRON Tensile Testing machine.

Once the tensile specimen was securely locked within the confines of the grips and the Blue Hill software program was completely set up with the desired parameters, a five minute run time of the digital multimeter is required to help stabilize the resistance readings coming from the CFF strain gauge. Two users are required for this experimental method to work. One person was designated to be the timer and responsible for activating the Agilent Benchvue program to record resistance data and the other person was responsible for activating the Blue Hill program to initiate the INSTRON tensile

machine. Prior to activation of the INSTRON tests, the user is required to press start of the Agilent Benchvue program to start recording the first five minutes of the resistance readings in order for it to reach a level of stabilization. After five minutes of stabilization time, both users need to coordinate the synchronization of this process so that one user actuates the INSTRON machine via the Blue Hill program and the other person is role is to use the timer to record the start of the tensile test run and time of fracture. The desired tensile rate dictated the duration at which the specimen will fracture. Once the tensile specimen fractures, the user will stop the program, and recorded the end time of the experiment. All the data in terms of resistance, stress, strain, max load, and time of fracture for each tensile rate experiment (1 mm/min and 0.7 mm/min) were recorded and exported to an excel spreadsheet for further analysis.

D. ELECTRICAL PROPERTIES DETERMINATION USING HARDWARE AND SOFTWARE ANALYSIS

To determine the electrical properties of the CFF strain gauge undergoing each type of tensile tests, the software program called Agilent Benchvue was used. An Agilent 34410A 6½ Digital Multimeter interacted with the Agilent Benchvue program via the computer's USB ports. The pair of lead wire clips of the Digital Multimeter were connected to the wires on each end of the CFF strain gauge of the tensile specimen, as shown in Figure 18. The wires on each end of the strain gauge element were connected to the Digital Multi-meter. The Agilent computer program recorded the resistance of the specimen throughout the tensile test runs. At the start of the test procedure, the sample was placed under increasing tension until it fractured. Upon completion, the MTESTQuattro program automatically saved the data, and was converted to Microsoft excel document for further analysis.

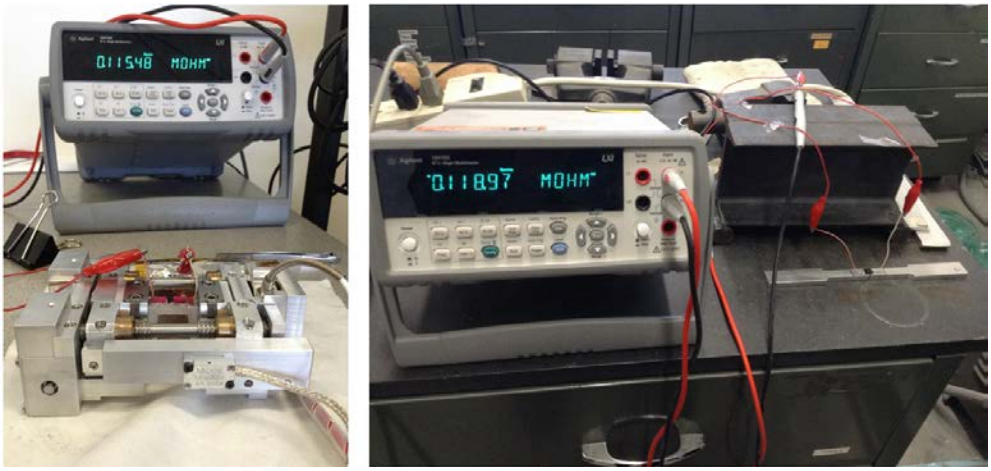

Figure 18. Each pair of wires were attached and embedded on top and bottom of the CFF strain gauge for Microtester specimen (left) and INSTRON tensile specimen (right), respectively, while the other end of pair of were connected to the Digital Agilent Multimeter.

E. MECHANICAL PROPERTY CHARACTERISTICS

(1) Microtester tensile test

Prior to conducting Microtester tensile test, it was important that the enclosure of the CFF strain gauge was constructed in a secure fashion in order for the foam inside the tube to be at a compressed state, as seen in Figure 23. This procedure initialized the resistance state of the foam. The reason for this method to be used was to maintain the CFF in a compression state during the entire test. Once the CFF becomes elongated relative to its initial size, the linear relationship between strain and resistivity is not maintained. The Microtester tensile stage was designed to exert tensile loads of up to 1000 lbs on a test specimen and to be installed in an SEM to observe microstructure of the sample as it is being stressed in tension. During each tensile run (0.001 in/min), MTESTQuattro program interacts with this device and records the stress, strain, and the max load of the specimen until it fractures.

(2) INSTRON tester

The mechanical properties of the CFF tensile specimen were evaluated by the use of the INSTRON 4507 tensile tester. This instrument was linked to a computer that contained the INSTRON Blue Hill program. The tensile rates that were inputted into the program that was used throughout the course of this experiment were 1 mm/min and 0.7 mm/min.

Upon completion of both types of tensile tests, the programs mentioned above allowed the user to record the tensile stress and strain at maximum load, and automatically produced graphical relationships of the tensile stress over time.

THIS PAGE INTENTIONALLY LEFT BLANK

III. RESULTS AND DISCUSSION

The experiments performed in this thesis were meant to determine the effectiveness of using the fabricated CFF as a sensing element of a strain gauge to detect crack propagation on Al5083 specimens. This chapter presents the results and data generated along with a discussion of the same in the following sequence: (A) CFF Growth and SEM microstructural analysis, (B) Construction of CFF strain gauge sensors (C) Mechanical and electrical data, and (D) Comparing CFF to commercial strain gauge sensors.

A. CFF GROWTH AND SEM MICROSTRUTRAL ANALYSIS

After conducting the (CoFFiN) process, a highly porous tridimensional foam was produced and was used as a sensing element on a strain gauge as shown in Figure 19.

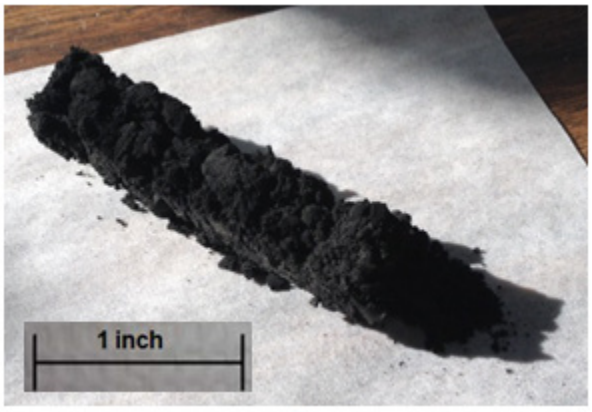

Figure 19. Successful growth of Carbon fiber foam on pure palladium.

As shown in SEM image of Figure 20, the fiber size ranged from approximately 50 nm to 200 nm in width. There were very few fibers with a diameter of less than 50 nm and the majority of them had diameters between 100 to 150 nm. Figure 20(A) illustrates how the foam is composed by fibers with void spaces in between. Studies by Daskam et al. show that the conductivity of the individual fibers is changed by strain [18]. The resistance changed as a function of strain because the number of contacts between fibers

increased with increasing strain, for example, when the foam is compressed, as in Figure 20(B). A compressive load would lead to more electrical paths, hence lower resistance.

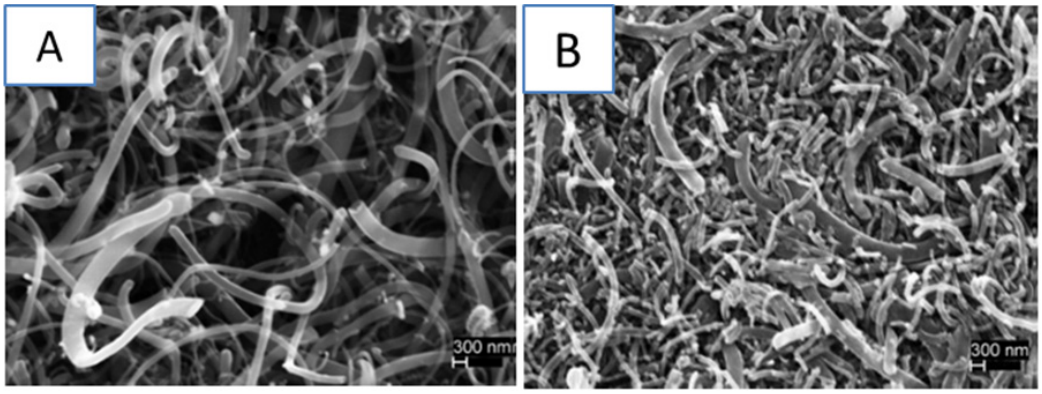

Figure 20. (A) Uncompressed CFF grown from palladium catalyst. (B) Compressed CFF showing a reduction of empty spaces in between fibers and more contacts among fibers.

B. CONSTRUCTION OF STRAIN GAUGE SENSORS

Eight strain gauge sensors were created for the Microtester Al5083 tensile specimens and six strain gauge sensors were created for the INSTRON tensile specimens. Each type of strain gauge sensors were created in the same dimensions according to what was delineated in the methods chapter. All the Al5083 tensile specimens were fabricated to have a notch in the middle in order to initiate crack propagation during each tensile test. As a result, the strain gauge sensors were placed right beside the tip of the notch on each tensile specimen.

As mentioned before, the sensors to be used with the microtester intended to reproduce a prototype of what a commercial sensor might look like. As such, it contained more elements than the ones placed for the Instron tester. The design for the microtester prototype included an enclosure to store the CFF, which will contain the foam in the transverse direction, but will allow it to freely move in the longitudinal direction. The ends of the prototype enclosure were attached to the Al5083 tensile specimen. The foam was supposed to be initially under compression to allow for larger strains to be achieved. The enclosure was comprised by two sleeves; the interior one was opened in the middle,

allowing for tensile test to be conducted, and an exterior sleeve, to contain the carbon foam, as shown in Figure 21.

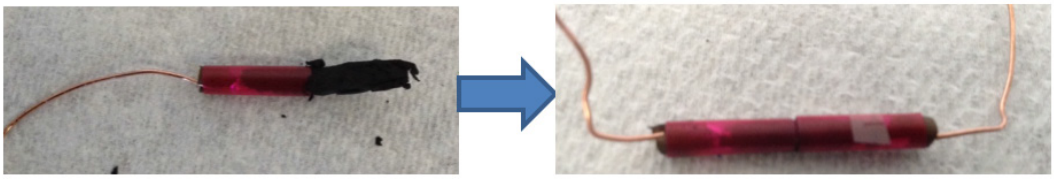

Figure 21. Fitting a tube of CFF into the polypropylene enclosure.

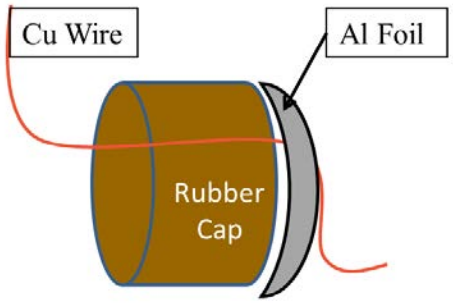

Figure 22. Inside schematic of one end of the CFF strain gauge of the Microtester tensile specimen.

The biggest challenge of constructing this type of sensor was to ensure that the CFF inside the enclosure was at maximum compressed state. This was an important step in the procedural process, because change in resistance will only occur linearly as the length changes up to the point that the CFF enters tension as seen in Figure 23. Part of the struggle for this sensor design was the difficulty of consistently cutting the right size of CFF to precisely fit into the enclosure and to introduce it in the cavity without breaking foam in the process. Furthermore, the copper wires provided the electrical connection within the enclosure. In order to have a good electrical signal through the rubber caps, aluminum foil served as interface with the conductive foam, as shown in Figure 22.

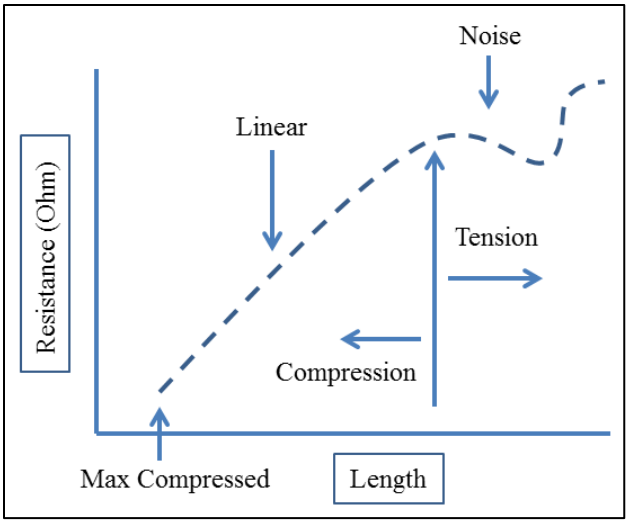

Figure 23. Schematic plot on the relationship of the CFF shape in terms of Length vs. Resistance.

Upon completion of constructing the CFF strain gauge sensor, the copper wires on each end of it were connected to a digital multimeter. A high level of inconsistent electrical resistance readings was discovered if the aluminum foil was not fitted securely within the enclosure causing a non-steady and erratic reading of electrical resistance. Despite the limitations with constructing this type of sensor, this prototype was attached to the Al5083 tensile specimen and underwent the Microtester tensile test to check if there was any significant change in the electrical resistance upon fracture of the tensile specimen.

In order to understand the operational principle of the foam, it becomes necessary to review how commercial strain gauges measure changes in electrical resistance as a function of the strain being applied and establish a correlation with the present case. The general principle of operation of a strain gauge is presented in Figure 24. Strain gauges entail the use of a thin wire or foil that is attached to a backing material, when a known level of stress is applied to the foil/wire its resistance changes so that the values of resistance can also be related to the corresponding strain levels. The relationship between strain and resistance of the sensor is known as the gauge factor.

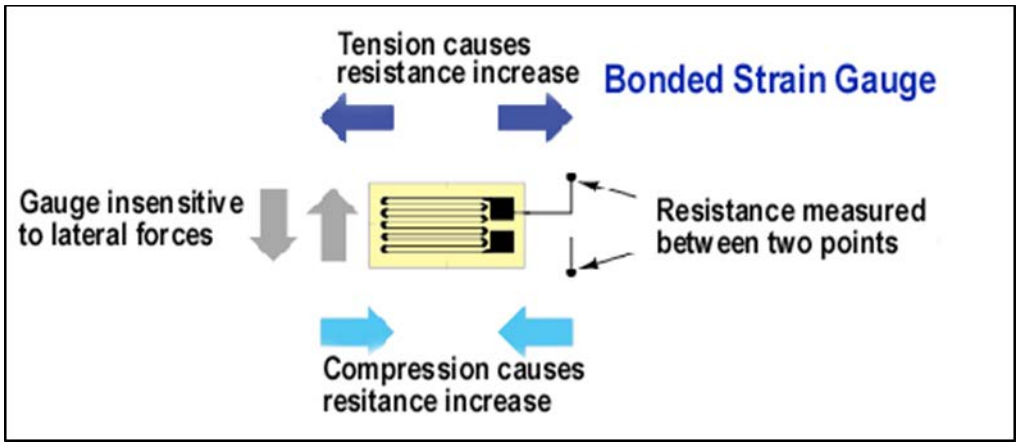

Figure 24. Diagram of a strain gauge, from [24].

Thus, the major metric for evaluating a strain gauge's sensitivity, is to have a high gauge factor (GF) [24]. This means that the change in resistance must be high relative to the change in strain [21], [24]. To determine the gauge factor, the following equation could be used:

$$GF = \frac{\Delta R / R_o}{\varepsilon}$$ from equation in reference [27]

DR represents the change in resistance, R_o its initial value and e the strain. The CFF foam has shown a gauge factor of approximately 0.6 [21], value obtained from the as shown below in Figure 24.

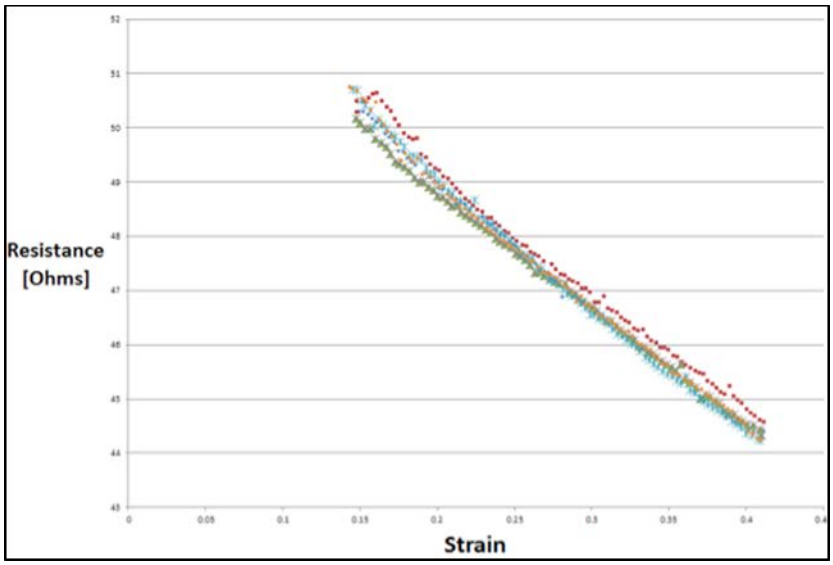

Figure 25. Linear relationship between resistance and strain in the CFF foam, from [23].

It is worth noting that the strain referred to in Figure 25 is that of the foam itself, measured during cyclic compression tests. The results presented in the sections ahead will attempt to relate the strain of the aluminum specimen subjected to tensile test with the resistance of the foam.

C. MECHANICAL AND ELECTRICAL DATA

Two computers were used to acquire the resistance and tensile data in these experiments; one computer was connected to the digital multimeter to record the electrical resistance and the other computer was connected to the INSTRON or Microtester tensile machine to record the mechanical data. Consequently, this method required precise synchronization of time for the two recording systems. Two people were required to perform this experiment in order activate each electrical and mechanical recording program on each computer.

Five minutes of stabilization time after pressing the activate/recording button of the Agilent Benchvue program was necessary to record steady resistance measurements. After the five minute mark, one person on the INSTRON computer was required to press the activate button to conduct the tensile test, while the other person operated the computer with the Agilent Benchvue program and used a timer to record the start/stop of

the experiment. This protocol proved to be a source of error in the data, since synchronization issues caused by operator could cause the timing to be off in a matter of seconds. An instrument that could trigger both measurements at the same instant is recommended for future research.

A limitation inherent of the Agilent Benchvue program should also be mentioned. The program will only record 60 minutes of the experiment. Any time beyond that, the program will stop recording data and a new set of data needed to be initiated. It was observed that the rates of 0.7 mm/min and 1.0 mm/min were the best conditional settings in order to record the electrical data within the required timeframe.

1. INSTRON Tensile Test Run (0.7 mm/min)

For this experimental run, the INSTRON machine was set for a tensile rate of 0.7 mm/min. The total time of the tensile run before fracture was four minutes and 54 seconds. The maximum load that the aluminum tensile specimen was able to withstand before fracture was 13,346 N. The tensile stress at maximum load was 243.89 MPa. Before the fracture point, the average resistance was 175.63 ohms. After fracture point, the max resistance yielded 306.15 ohm. The two trends between the resistance and load of the plot are used as indicators for a potential crack propagation to exist on the Al5083 specimen. The following figures illustrate the CFF performance as a strain gauge in terms of resistance and load or strain, over time.

Figure 26 illustrates the relationship between Resistance vs. Time and Load vs. Time of the CFF strain gauge under tensile stress until the point of fracture. As more tensional load is being imposed on the Al5083 specimen, the resistance gradually increases. Before the point of fracture the resistance will drop and then exponentially increase when the fracture fully occurs.

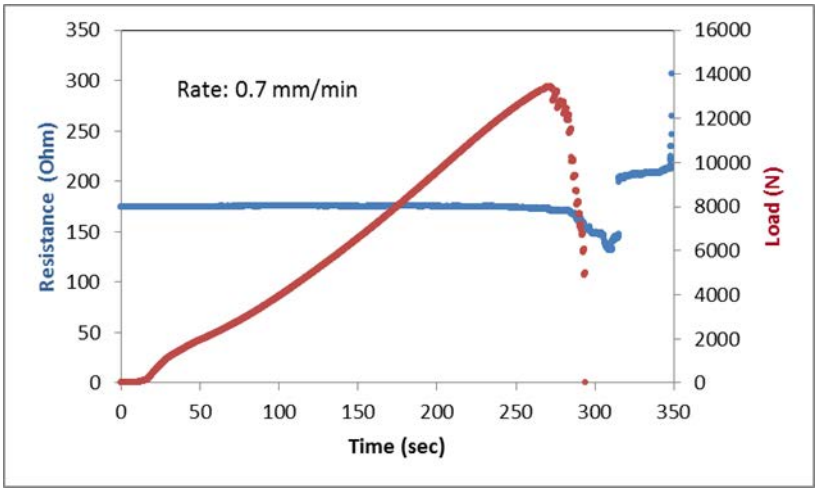

Figure 26. Resistance Vs. Time (blue plot) and Load vs. Time (red plot) relationship for CFF strain gauge specimen undergoing tensile rate of 0.7 mm/min.

Figure 27 illustrates the relationship between the Resistance vs. Time and Strain vs. Time under tensile stress until the point of fracture. The blue plot is the same data points as the graph depicted in Figure 26. In this tensile run, the red plot illustrates that the strain of the CFF specimen increases linearly over time until the point of fracture. During the fracture transient sequence, the resistance gradually decreases and then it exponential increases until the CFF tensile specimen completely splits apart.

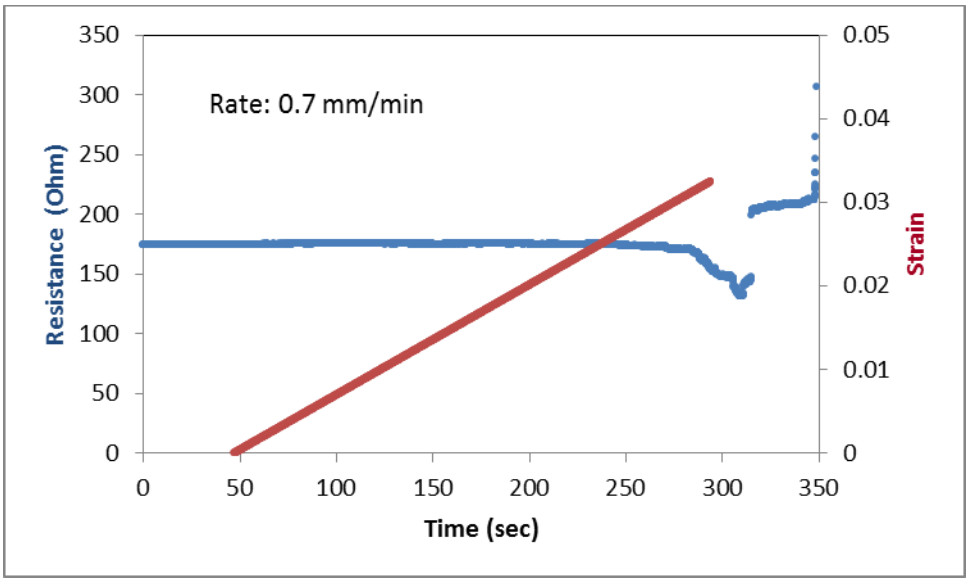

Figure 27. Resistance vs. Time (blue plot) and Strain vs. Time (red plot) relationship for CFF strain gauge specimen undergoing tensile rate of 0.7 mm/min.

2. INSTRON Tensile Test Run (1.0 mm/min)

In this experimental run, the INSTRON machine was set for a tensile rate of 1.0 mm/min. The total time of the tensile run before fracture was five minutes and 17 seconds. The maximum load that the tensile specimen was able to withstand before fracture was 10921 N. The tensile stress at maximum load was 204.66 MPa. Before the fracture point, the average resistance was 212.78 ohms. After fracture point, the max resistance yielded 12455.45 ohm. The following are two double axis graphs that illustrate a similar CFF performance as a strain gauge in terms of resistance and load, or strain over time.

In Figure 28 shows the comparison between the resistance and load trend of the CFF strain gauge specimen over time. As the load increases over time, the resistance stays at a steady rate. Similar to the reaction from the fracture point from Figure 26, the resistance steadily drops and then exponentially increases after the CFF tensile specimen has completely fractured.

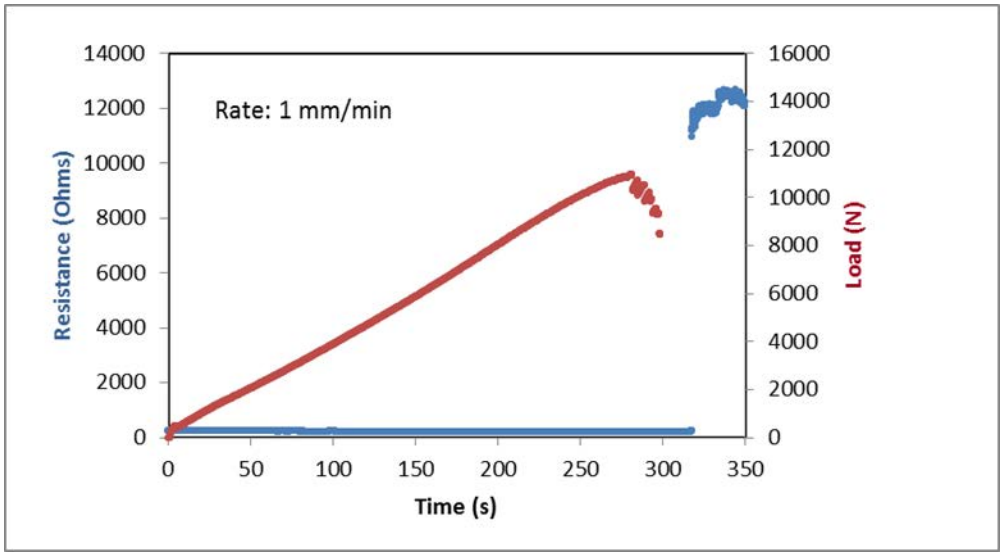

Figure 28. Resistance vs. Time (blue plot) and Load vs. Time (red plot) relationship for CFF strain gauge specimen undergoing tensile rate of 1.0 mm/min.

Figure 28 illustrates the relationship between the Resistance vs. Time and Strain vs. Time under tensile stress until the point of fracture. In this tensile run, similar to the behavior trend shown in Figure 27, that the strain of the CFF specimen increases linearly over time until the point of fracture. During the fracture transient sequence, the resistance gradually decreases and then it exponential increases until the CFF tensile specimen completely splits apart.

It is worth mentioning that when compared, runs at different strain rates demonstrate that slower test rates are able to capture smaller changes in resistance before the final step increase in the resistance values, as is the case on the 0.7 mm/min runs. Higher strain rates show mainly a single step increase that correlates with the final aluminum tensile specimen fracture.

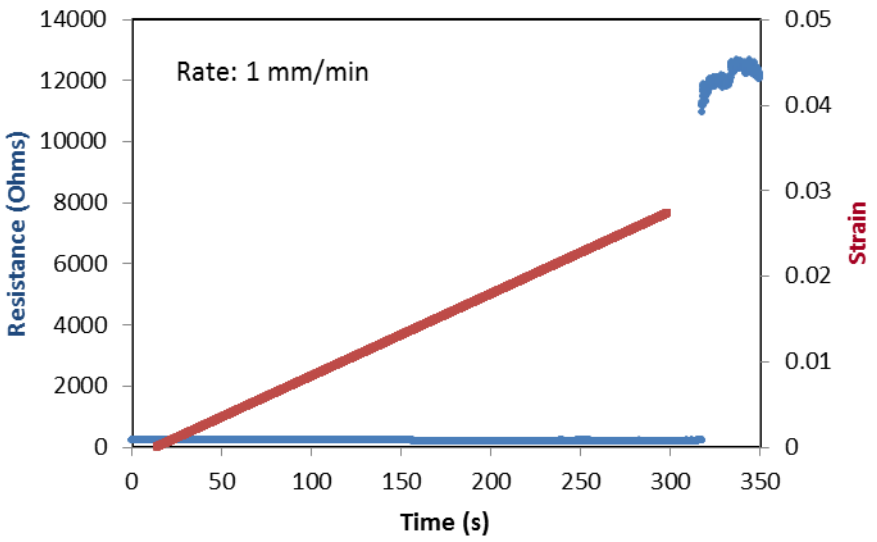

Figure 29. Resistance Vs. Time (blue plot) and Strain vs. Time (red plot) relationship for CFF strain gauge specimen undergoing tensile rate of 1.0 mm/min.

Overall, the general trend between strain and resistance of the CFF is that resistance decreased with increased strain. All four of these plots indicate that resistance can be correlated to strain. For the INSTRON tensile runs, the CFF performs in a linear fashion at least a 3% strain. Daskam et al. observed in this experimental compression tests that CFF performs linearly to at least 40% strain [21]. From comparing this two strain values, it can be inferred that CFF can be best used in cases where the anticipated change in strain is greater than 3%. The major differences observed between previous tests and the ones represented in Figures 26 to 29, is that there seems to be a slight mismatch between the strain observed in the aluminum structure and the ones (not recorded in here) that correspond to the foam.

The GF was calculated using the resistance and strain data points collected from the plots from Figure 27 and 29, resulting in values of approximately four. As mentioned above, such value does not represent the GF of the foam but a combined effect of tensile specimen strain and foam. Moreover, since the foam gauges finish fracturing along the tensile specimens, the loss in resistance is related to have less connection between fibers not only due to voids in the structure but a complete loss in the connectivity of the

sample. The gauge factor for the combined runs are lower than the common material used on commercial strain gauges shown in Table 1. After obtaining the gauge factor, the anticipated change in resistance can be calculated for any range of strain. For example, for the two INSTRON tensile test runs, with a 3% strain and GF of 0.6, the anticipated final resistance was calculated to be 178.15 Ohms and 221.62 Ohms, respectively. Therefore, the change of resistance was ~2% which is less than 3% strain. This low gauge factor implies that CFF strain gauge can be more effective in detecting crack growth only if the resistance change is higher than the given strain. Further test will be certainly necessary to determine if CFF strain gauge can be better utilized as a tool to monitor crack growth after the initial crack formation.

The most successful specimens tested consisted of the foam encased on three layers of nitrocellulose, which provided electrical isolation for the foam in the absence of movable sleeves.

Table 1. General examples of commercial strain gauges and respective gauge factors, from [27].

Material	Gauge Factor
Metal foil strain gauge	2-5
Thin-film metal (e.g. Constantan)	2
Single crystal silicon	-125 to + 200
Polysilicon	±30
Thick-film resistors	100

Despite the need to improve and optimize the CFF-based strain sensors, we could see a correlation between crack propagation on Aluminum structures and resistance of the foam specimens, providing a proof of concept for the hypothesis presented.

D. COMPARING CFF TO COMMERCIAL STRAIN GAUGE SENSORS

One example of a commercial strain gauge that was used prior to executing the CFF strain gauge tensile tests mentioned in the previous experimental chapter was the use of Omega brand Strain Gauge. This particular strain gauge requires the use SG401 rapid cure adhesive. When this strain gauge was applied on the small dimensional Al5083 specimen and ran through the Microtester tensile test, the strain gauge delaminated from the Al specimen prior to the point of fracture. Furthermore, the dimensions of the gauge are quite small. If the placement is not perfect, little strain will occur "under" the gauge. In fact, no electrical signal was detected from the commercial gauge, either before or after the "dog bone" broke. This serves as an example of a disadvantage of using commercial strain gauge on structures. The strain gauge is only sampling a very small part of the structure. It is not large enough to provide a meaningful "averaged" reading. Furthermore, CFF does not need binders, polymeric matrices, or linking additives to form 3D structures of selected shape. Hence, the CFF strain gauge can be made from a sensing material of any size and can be fitted to any dimensional structure of interest in order to be used as a potential structural health monitor of detecting growth of cracks on metal structures.

THIS PAGE INTENTIONALLY LEFT BLANK

IV. CONCLUSIONS

We determined that carbon-nano fibers foams, based on their electrical response to diverse levels of strain, can be used as gauge sensors to detect crack propagation in aluminum structures.

We were able to integrate carbon nano-fiber foams with aluminum plates using polymeric encasings that provided electrical insulation. Such prototypes produced simultaneous mechanical and electrical data. However, we found certain challenges during the construction of the same that will need to be addressed to produce consistent readings.

We assessed the foam's sensitivity (strain gauge factor) to micro crack propagation, obtaining values that vary between 0.6 for bare foam to four for the combined foam-Al plate.

We found that the use of the carbon fiber foam as strain gauge presents advantages over the commercially available sensors.

Out of the two prototypes, the macro design for testing the INSTRON aluminum specimen was more successful in proving the concept. The use of nitrocellulose was an effective adhesion to keep the CFF electrically insulated while keeping the foam at a maximum compressed state. The INSTRON tensile method proved the most effective electrical-mechanical test to evaluate the CFF's conductivity and sensitivity to different levels of strain. The behavior relationship between resistance and strain are helpful indicators of showing time of crack initiation.

The CFF microtester strain gauge prototype design was a step in the right direction in determining if the foam can be integrated effectively as a strain sensor. Further refinement is needed to keep the CFF at a maximum compressed state prior to tensile testing and keeping the Al foil and wire configuration fitted securely within the polypropylene enclosure to produce the proper state of conductivity of the CFF during tensile testing.

With time and a few refinements, this CFF strain gauge can be of great use as a structural health monitor onboard naval vessels on providing timely warning detection of incipient damages present in structures, resulting in the prevention of catastrophic structural failures and help reduce maintenance cost in the U.S. Navy.

V. RECOMMENDATIONS FOR FUTURE RESEARCH

Future work should focus on improving the construction of the CFF enclosure design prototype. Better software synchronization in terms of data/time recording should be implemented to correct the errors that were presented in this manuscript.

Each type of CFF strain sensor design, different ranges of temperature conditions should be used during the experiment in order to check if temperature has any bearing on the sensitivity of the CFF material as a strain gauge.

The gauge factor of the CFF is very small and efforts to increase it should be considered for future work.

THIS PAGE INTENTIONALLY LEFT BLANK

APPENDIX A. MICROTESTER TENSILE TEST PROCEDURE

MATERIALS AND EQUIPMENT

- SEM Tester
- Gloves
- Caliber
- Specimen of interest

PROCEDURE AND SET UP

- Turn on Computer. Turn On Black Control Box. Log-in Computer.
- Username: student
- Password: ABCabc..123
- Open up MTEST Quatro program
- Go to File → New → Test Procedures

Under Specimen Tab, input the following parameters:

- Type : Flat
- Identifier: Input Name of Specimen
- Geometry Units: inches
- Axial Strain Gauge Length(in.): 0.756
- Transverse Strain Gauge Length (in): 1.0
- Grip Separation (in.): 0.0
- Flat Geometry Parameters:
- Width (in.): 0.19
- Thickness(in.): 0.053

Under Report Setup Tab, input the following parameters:

- Title: Enter desired Title name of experiment
- Comments: Enter any necessary comments/information about specimen
- Check mark “Include Plot When Reporting Results
- Report Parameters: Enter Label & Value

Under Acquisition tab, enter the following parameters:

- Threshold Channel: Load
- Threshold Value (lb): 0.0
- Logging Cutoff: Stop at End of Profile
- Check marked “Freeze Strain Channels at Yield”
- Load Threshold(lb): 200.0
- Save Options: Autosave Test Data
- Prefix: User Profile
- Prefix: Enter desired filename and date
- Test Results Name: Use Entered Name
- Type filename and date
- Check marked “Autoadd Analysis Calculations to Test Results
- Select “Never”

Under Analysis Tab, enter the following parameters:

- No need to select Available Analyses
- Elastic Slope Calculation: Automatic

Under XY Graph Tab, enter the following parameters:

- Y-Axis:
- Channel: Stress
- High Scale (psi): 0.032
- Low Scale (psi): 0.0
- Divisions: 4
- X-Axis:
- Channel: Position
- High Scale (in.): 0.25
- Low Scale (in.): 0.0
- Divisions: 4
- Plot Options
- Scaling: Auto Scale

Under Channel tab, enter the following parameters:

- Transducer: Select 1411034 1000lb Tension
- Units:
- Load: lb
- Stress: psi
- Position: in
- Rate Units
- Load: sec
- Stress: sec
- Position: sec

Under Servo Control tab, input the following parameters:

- Preload (lb): 0.5
- Preload (in/min): 0.001
- Jog Rate (in/min): 0.001
- Home Rate (in/min): 0.1
- Select Offset from Zero
- End-of-Test Action: Stop at End-of-Test
- Overload Range (lb): 1005.0
- Rate Units: in
- Rate Interval: min

Put white Table cloth underneath SEM Tester
Input the specimen into the middle slot of SEM Tester

- Use High Vacuum grease to better secure the small input block onto SEM Tester platform.
- Use an allen wrench to tighten the bolts to secure specimen.

Press “Home” icon to initialize the SEM Tester.
Press “Play” on the program to start SEM Tester. Expect to hear a “hissing sound.” This is indication that the SEM Tester is working and is executing the proper mechanical test. Simultaneously, the MTEST Quatro program will project a stress/strain curve of the experiment.
When finished, press “stop” button. Save Data Results by pressing the Floppy disk icon.

- Under Test Data folder, right Click, export and save to desire file directory location.
- Open data in Excel
- Create data table and desired plots
- Generate the stress/curve plot from the excel data and generate the proper stress vs. strain curve.

After accumulating the necessary data. Press “Home” button to restart and retract the SEM Tester to its starting position.

- After test is over, remove the specimen from the SEM Tester by removing the screws using the allen wrench. Place the blocks and screws back together and secure SEM Tester device.

APPENDIX B. INSTRON TENSILE TEST PROCEDURE

1. Connect the extensometer to INSTRON frame. The connection port is located the back of INSTRON frame and labeled “Extensometer.”
2. Power up the load frame.
3. Turn on the computer.
4. Double click on the Instron BLUEHILL Icon. This starts the loading of Bluehill software.
5. After a few seconds the Bluehill Home Screen appears.
6. Checks the frame enables blue light
7. Adjust the crosshead for your sample by using jog up, jog down, and fine position knob
8. Load your sample into Grips.
9. From the Home screen, check the load cell position for correct test.
10. From the Home screen Click on the Method Icon that is the second icon from the top.
11. Click on the New Button from the Button Bar on the right.
12. Select the appropriate Test Type, Tension for this example and Click the Create button.
13. Setting General Parameters that depend on your test such as method, sample, basic layout, and advanced layout.
14. Setting Specimen Parameters of your sample such as dimensions, number inputs, text inputs, and notes.
15. Setting Control Parameters of your test.
    - Test: tensile test or compression test.
    - End of Test: stop the machine when test is done.
    - Data: data collecting rate and the number of data points.
    - Strain: strain rate for test.
16. Defining Results Tables. This table will show all information that you want to know.
17. Defining Graphs that you want to see the graph. You can set up the type, X axis data, and Y axis data of the graphs.
18. Save the Method as your name for your own test.
19. Attach the extensometer on to sample.

    Caution: The extensometer is very delicate instrument so you have to handle very carefully.
20. Go to Test Icon for running a test.
21. Click the test icon in the home screen.
22. Select a method for your test. Make sure that the test is correct test for you.

23. Create the sample file name.
24. Click the load icon.
25. Balance the load to zero.
26. Click the gage length (GL) icon.
27. Balance the GL to zero.
28. Click the extensometer icon.
29. Balance the extensometer.
30. Click the start icon for stating the mechanical test.
31. After the test, click the finish icon and save all tested data.

LIST OF REFERENCES

[1] R. Schwarting, G. Ebel, and J. Dorsch, "Manufacturing techniques and process challenges with CG47 class ship aluminum superstructure modernization and repairs," *BAE Systems, Norfolk, VA*, 2011.

[2] R. S. Matthew Collette, "Aluminum ship structures," *Appl. Phys. Lett.*, pp. 1–14, 2005.

[3] E. Fakhouri, "Systematic review of ultrasonic impact treatment parameters on residual stresses of welded non-sensitized versus sensitized aluminum-magnesium," M. S. thesis, Dept. Mech. Eng. , Naval Postgraduate School, Monterey, CA, 2014.

[4] M. Haggett, "Systematic Review of UIT parameters on residual stresses of sensitized AA5456 and field-based residual stress measurements for predicting and mitigating stress corrosion cracking," M. S. thesis, Dept. Mech. Eng. , Naval Postgraduate School, Monterey, CA, 2014.

[5] *USS Bunker Hill* (CG-52). (May 05, 2011). Available: http://www.c7f.navy.mil/imagery/galleries/monthly/2011/05-May/index10.htm

[6] *LCS*. (AUG 8, 2008). Available: http://www.naval.com.br/blog/wp-content/uploads/2008/08/lcs-sea-trials-2.jpg

[7] M. G. Fontana, *Corrosion Engineering.* New York, NY: McGraw-Hill Book Company, 1987.

[8] R. Goswami *et al.*, "Microstructural evolution and stress-corrosion cracking behavior of al-5083," in *Metallurgical and Materials Transactions* Anonymous 2011, pp. 348–355.

[9] I. Oguocha and O. Adigun, "Effect of sensitization heat treatment on properties of Al-Mg alloy AA5083-H116," *Journal of Material Sci.*, vol. 43, pp. 4208–4214, 2008.

[10] *Alloy Phase Diagram Database*. (Feb. 14, 2014). Available: http://www1.asminternational.org.libproxy.nps.edu/asmenterprise/APD/ViewAPD.aspx?id=101029

[11] E. C. Cormack, "The effect of sensitization on the stress corrosion cracking of aluminum alloy 5456," M. S. thesis, Dept. Mech. Eng., Naval Postgraduate School, Monterey, CA, 2012.

[12] W. D. Callister, *Materials Science and Engineering: An Introduction.* York, PA: John Wiley and Sons, Inc, 2007.

[13] B. Ayyub, I. Assakkaf, and D. Kihl, “Reliability-based design guidelines for fatigue of ship structures,” *Journal of Structural Engineering,* vol. 113, pp. 280–283, October 29, 2008.

[14] R. Sielski, K. Nahshon, L. Salvino, K. Anderson, and R. Dow, “The ONR Ship Structural Reliability Program,” *American Society of Naval Engineers,* pp. 1–28, February 12, 2012.

[15] J. Ihn and F. Chang, “Detection and monitoring of hidden fatigue crack growth using a built-in piezoelectric sensor/actuator network,” *IOP Science,* pp. 609–620, 2004.

[16] K. Karimov, M. Saleem, Z. Karieva, A. Khan, T. Qasuria and A. Mateen, “A carbon nanotube-based pressure sensor,” *Physica Scripta,* pp. 1–4, 14 April, 2011.

[17] A. Sethi, “Structural health monitoring of steel structures using electrical strain gauges,” *Indian Institute of Technology Delhi,* pp. 1–13, 2003.

[18] J. Phillips, “Mechanical and electrical characterization of entangled networks of carbon nanofibers,” in *Carbon Fibers,* 2015th ed., J. Phillips, Ed. MDPI, Basel, Switzerland: Shu-Kun Lin, 2015, pp. 91–99.

[19] T. L. Sida Luo, “Structure-property-processing relationships of single-wall carbon nanotube thin film piezoresistive sensors,” *SciVerse ScienceDirect,* pp. 315–324, 21 March, 2013.

[20] C. Su, C. Li, N. Chang, F. Gao and S. Chang, “Fabrication of high sensitivity carbon microcoil pressure sensors,” *Sensors,* pp. 35–41, 25 July, 2012.

[21] J. Phillips, T. Shiina, M. Nemer, and K. Lester, “Graphitic structure by design,” *American Chemical Society,* August 10, 2006.

[22] G. Tibbetts, M. Lake, K. Strong and B. Rice, “A review of the fabrication and properties of vapor-grown carbon nanofiber/polymer composites.” *Composites Sci. Technol,* vol. 67, pp. 1709–1718, 2007.

[23] D. C. Daskam, “Fabrication of a low density carbon fiber foam and its characterization as a strain gauge,” M. S. thesis. Naval Postgraduate School, Monterey CA, 2013.

[24] *Strain Gauge*. (April 7, 2010). Available: http://www.circuitstoday.com/strain-gauge.

[25] N. Hu, “Investigation on sensitivity of a polymer/carbon nanotube composite strain sensor,” *Carbon,* vol. 48, pp. 680–687, Mar 2010.

[26] E. Minot, “Tuning carbon nanotube band gaps with strain,” *Phys. Rev. Lett.*, vol. 90, pp. 157–601, Feb 2005.

[27] *The Strain Gauge*. (18 May 2015). Available: http://www.omega.com/literature/transactions/volume3/strain.html

THIS PAGE INTENTIONALLY LEFT BLANK

INITIAL DISTRIBUTION LIST

1. Defense Technical Information Center
   Ft. Belvoir, Virginia

2. Dudley Knox Library
   Naval Postgraduate School
   Monterey, California